grained rocks (granite). We used samples from the 22 sites to measure the angle α between pairs of striations. At every site, well-defined striation angles were measured on a number of samples. As predicted, the angles measured within an individual sample are relatively constant with a typical standard deviation of 5° (Fig. 4b). In addition, the mean striation angles systematically increase from 17° to 46° with the distance from the impact centre (Fig.4c). Thus, both the narrow angular distributions and the systematic increase of mean angles are consistent with our postulate that the striations are formed by front waves.

Using $\cos(\alpha/2) = V/V_{FW} \approx V/V_R$, we calculated the fracture velocities from the measured angles (Fig. 4c). The specific values of V_R in the samples are immaterial, because the angle α measures only the normalized fracture velocity, V/V_{FW}. We find that V approaches $0.98V_R$ at approximately 15 km from the impact centre, and decreases to $\sim 0.9V_R$ at 35–40 km from the centre. Thus, shatter cones are observed within the narrow range of fracture velocities above $0.9V_R$. Using the calculated spatial distribution of the stress applied by the shock wave at Vredefort[4], Fig. 4d indicates a precipitous rise of the applied stresses with fracture velocity. This increase is consistent with laboratory experiments[29] at lower velocities, and amply demonstrates why mean fracture velocities approaching V_R are never observed in the laboratory. At the larger striation angles, we find that shatter cones are not as easily recognized, as clear striations are less frequently observed, possibly because their amplitudes are reduced at lower energy flux levels.

We have shown that shatter cones are branched tensile fractures. Shatter-cone striations are the preserved tracks of fracture front waves. Analysis of the striations shows that shatter cones develop only at extreme propagation velocities, between $0.9V_R$ and the maximal permitted velocity of V_R. The angles of the striations (α), which are shown to increase systematically with the distance from the impact, reflect both the stresses and the energy flux driving the fracture at a given site, and may be used as a general tool to evaluate extreme local stresses in the field. Our results also demonstrate that such rapid fracture propagation in intact solids necessitates extremely high-energy fluxes, supplied naturally only by large impactors. □

Received 5 February; accepted 10 June 2002; doi:10.1038/nature00903.

1. Melosh, H. J. Impact ejection, spallation, and the origin of meteorites. *Icarus* **59,** 234–260 (1984).
2. Melosh, H. J. *Impact Cratering: A Geologic Process* (Oxford Univ. Press, New York, 1989).
3. French, B. M. *Traces of Catastrophe. Handbook of Shock-metamorphic Effects in Terrestrial Meteorite Impact Structures* (Lunar and Planetary Institute, Houston, 1998).
4. Turtle, E. P. & Pierazzo, E. Constraints on the size of the Vredefort impact crater from numerical modeling. *Meteorit. Planet. Sci.* **33,** 483–490 (1998).
5. Dietz, R. S. in *Shock Metamorphism of Natural Materials* (eds French, B. M. & Short, N. M.) 267–285 (Mono Book Corp., Baltimore, 1969).
6. Sharpton, V. L., Dressler, B. O., Herrick, R. R., Schnieders, B. & Scott, J. New constraints on the Slate Islands impact structure, Ontario, Canada. *Geology* **24,** 851–854 (1996).
7. Morrissey, J. W. & Rice, J. R. Crack front waves. *J. Mech. Phys. Solids* **46,** 467–487 (1998).
8. Morrissey, J. W. & Rice, J. R. Perturbative simulations of crack front waves. *J. Mech. Phys. Solids* **48,** 1229–1251 (2000).
9. Ramanathan, S. & Fisher, D. S. Dynamics and instabilities of planar tensile cracks in heterogeneous media. *Phys. Rev. Lett.* **79,** 877–880 (1997).
10. Sharon, E., Cohen, G. & Fineberg, J. Propagating solitary waves along a rapidly moving crack front. *Nature* **410,** 68–71 (2001).
11. Milton, D. J. in *Impact and Explosion Cratering; Planetary and Terrestrial Implications* (eds Roddy, D. J., Pepin, R. O. & Merrill, R. B.) 703–714 (Pergamon, New York, 1977).
12. Roy, D. W. Shatter cone geometry and description procedure. *Tectonophysics* **60,** T37–T42 (1979).
13. Albat, H. M. & Mayer, J. J. Megascopic planar shock fractures in the Vredefort Structure; a potential time marker? *Tectonophysics* **162,** 265–276 (1989).
14. Nicolaysen, L. O. & Reimold, W. U. Vredefort shatter cones revisited. *J. Geophys. Res. B* **104,** 4911–4930 (1999).
15. Johnson, G. P. & Talbot, R. J. *A Theoretical Study of the Shock Wave Origin of Shatter Cones* Thesis (Air Force Inst. Technol., Wright-Patterson Air Force Base).
16. Gash, P. J. S. Dynamic mechanism for the formation of shatter cones. *Nature* **230,** 32–35 (1971).
17. Shibuya, T. & Nakahara, I. The semi-infinite body subjected to a concentrated impact load on the surface. *Bull. Jpn Soc. Mech. Eng.* **11,** 983–992 (1968).
18. Asphaug, E. *et al.* Mechanical and geological effects of impact cratering on Ida. *Icarus* **120,** 158–184 (1996).
19. Camacho, G. T. & Ortiz, M. Computational modelling of impact damage in brittle materials. *Int. J. Solids Struct.* **33,** 2899–2938 (1996).
20. Melosh, H. J., Ryan, E. V. & Asphaug, E. Dynamic fragmentation in impacts — Hydrocode simulation of laboratory impacts. *J. Geophys. Res. E* **97,** 14735–14759 (1992).
21. Field, J. E. Brittle fracture: its study and application. *Contemp. Phys.* **12,** 1–31 (1971).
22. Ahrens, T. J. & Rubin, A. M. Impact-induced tensional failure in rock. *J. Geophys. Res. E* **98,** 1185–1203 (1993).
23. Polanskey, C. A. & Ahrens, T. J. Impact spallation experiments; fracture patterns and spall velocities. *Icarus* **87,** 140–155 (1990).
24. Arakawa, M., Shirai, K. & Kato, M. Shock wave and fracture propagation in water ice by high velocity impact. *Geophys. Res. Lett.* **27,** 305–308 (2000).
25. Sharon, E. & Fineberg, J. Microbranching instability and the dynamic fracture of brittle materials. *Phys. Rev. B* **54,** 7128–7139 (1996).
26. Sagy, A., Reches, Z. & Roman, I. Dynamic fracturing; field and experimental observations. *J. Struct. Geol.* **23,** 1223–1239 (2001).
27. Freund, L. B. *Dynamic Fracture Mechanics* (Cambridge Univ. Press, Cambridge, 1990).
28. Henkel, H. & Reimold, W. U. Integrated geophysical modelling of a giant, complex impact structure; anatomy of the Vredefort Structure, South Africa. *Tectonophysics* **287,** 1–20 (1998).
29. Dally, J. W. Dynamic photoelastic studies of fracture. *Exp. Mech.* **19,** 349–361 (1979).
30. Therriault, A. M., Grieve, R. A. F. & Reimold, W. U. Original size of the Vredefort Structure; implications for the geological evolution of the Witwatersrand Basin. *Meteorit. Planet. Sci.* **32,** 71–77 (1997).

Acknowledgements

We thank W. U. Reimold and E. G. Charlesworth for information and hospitality at the Vredefort site; the Rogers Group's Newton County quarry for their hospitality at the Kentland site; and G. Cohen for assistance. This work was supported by the United States–Israel Binational Fund.

Competing interests statement

The authors declare that they have no competing financial interests.

Correspondence and requests for materials should be addressed to J.F. (e-mail: jay@vms.huji.ac.il).

Climate-mediated energetic constraints on the distribution of hibernating mammals

Murray M. Humphries*†, Donald W. Thomas‡ & John R. Speakman*§

* *Department of Zoology, University of Aberdeen, Aberdeen AB24 3TZ, UK*
† *Department of Biological Sciences, University of Alberta, Edmonton, Alberta T6G 2E9, Canada*
‡ *Département de Biologie, Université de Sherbrooke, Sherbrooke, Québec J1K 2R1, Canada*
§ *Rowett Research Institute, Bucksburn, Aberdeen AB21 9BS, UK*

To predict the consequences of human-induced global climate change, we need to understand how climate is linked to biogeography[1]. Energetic constraints are commonly invoked to explain animal distributions, and physiological parameters are known to vary along distributional gradients[2]. But the causal nature of the links between climate and animal biogeography remain largely obscure[2,3]. Here we develop a bioenergetic model that predicts the feasibility of mammalian hibernation under different climatic conditions. As an example, we use the well-quantified hibernation energetics of the little brown bat (*Myotis lucifugus*) to parameterize the model[4]. Our model predicts pronounced effects of ambient temperature on total winter energy requirements, and a relatively narrow combination of hibernaculum temperatures and winter lengths permitting successful hibernation. Microhabitat and northern distribution limits of *M. lucifugus* are consistent with model predictions, suggesting that the thermal dependence of hibernation energetics constrains the biogeography of this species. Integrating projections of climate change into our model predicts a pronounced northward range expansion of hibernating bats within the next 80 years. Bioener-

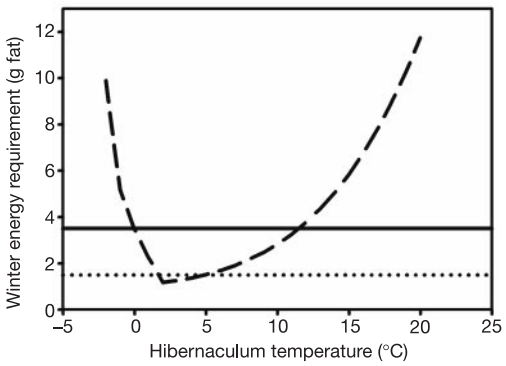

Figure 1 The effect of hibernaculum temperature on total winter energy requirements of *M. lucifugus* (dashed line), based on a winter length of 193 days[10]. The horizontal lines indicate approximate maximum (solid line) and minimum (dotted line) hibernation fat stores[9].

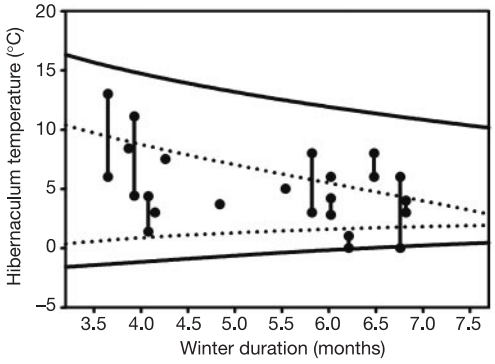

Figure 2 Comparison of observed hibernaculum temperatures of *M. lucifugus* with those predicted to be suitable by the model. Combinations of winter length and hibernaculum temperatures above the upper solid line or below the lower solid line are predicted to require more than the maximum fat stores (3.5 g)[9] to survive winter. Combinations above or below the dashed lines require more than minimum fat stores (1.5 g)[9]. Circles represent recorded hibernaculum temperatures of *M. lucifugus* at different geographical locations, and circles connected by a line represent a range of occupied temperatures reported from a single location[10,19–28]. Winter duration for each location is estimated from the period when nightly minima are below 0 °C. Most hibernacula are characterized by temperatures predicted to permit successful hibernation with minimum fat stores (12 of 15), and all are characterized by temperatures permitting successful hibernation with maximum fat stores (15 of 15). Maximum occupied temperatures are significantly lower than maximum suitable temperatures (Student's paired $t_{15} = 10.8$, $P < 0.0001$) and minimum occupied temperatures are significantly higher than minimum suitable temperatures (paired $t_{15} = 6.1$, $P < 0.0001$).

getics can provide the simple link between climate and biogeography needed to predict the consequences of climate change.

Explanation of the geographic distribution of organisms is a central aim of ecology[5]. Climate is clearly involved, because distribution limits frequently match climatic features such as seasonal minimum or maximum temperature isotherms[6]. Nevertheless, the mechanisms that underlie these patterns remain obscure[2,3,7]. In many cases, the ability of species to occupy a given environment may be determined by seasonal energetic bottlenecks within the annual cycle[8]. In these situations, explanation of distribution limits using climate-based energetic models may be much simpler than previously recognized[3]. For example, over-winter survival of hibernating mammals should depend primarily on the size of their energy reserves at the onset of hibernation, the rate at which the energy store is depleted during winter, and the length of the winter. If the size of the reserve is less than the rate of depletion times the length of winter, the hibernator will not survive. Here, we model the quantitative relationship between ambient temperature and energy expenditure during hibernation for a common North American bat, then combine this with estimates of winter length and the maximum size of fat stores to predict under what climatic conditions successful hibernation should be possible.

We focus this modelling approach on *M. lucifugus* because of the availability of empirical data on its hibernation energetics and distribution patterns, and the relative ease of predicting the thermal

Box 1
Temperature and hibernation energetics

The energy expenditure of an endotherm with a normal, elevated body temperature (euthermic), E_{eu}, varies with ambient temperature, T_a, according to a well-described metabolic response curve:

$$E_{eu} = RMR + (T_{lc} - T_a)C_{eu}$$

where *RMR* is resting metabolic rate, T_{lc} is the lower critical temperature, and C_{eu} is euthermic thermal conductance[30]. During torpor, metabolic rate, *TMR*, and body temperature decline with T_a until a lower ambient set-point temperature, $T_{tor\text{-}min}$, is reached, after which torpor body temperature is defended (that is, remains constant) and consequently *TMR* increases. Thus, *TMR* varies with temperature according to

$$E_{tor} = TMR_{min} Q_{10}^{(T_a - T_{tor\text{-}min})/10}, \quad \text{if } T_a > T_{tor\text{-}min}$$

$$E_{tor} = TMR_{min} + (T_{tor\text{-}min} - T_a)C_t, \quad \text{if } T_a \le T_{tor\text{-}min}$$

where Q_{10} represents the change in torpor metabolism resulting from a 10 °C change in T_a, and C_t represents torpor conductance below $T_{tor\text{-}min}$.

All mammalian hibernators arouse from torpor at regular intervals during winter, remaining euthermic for a short time before re-entering torpor[30]. The energetic cost of these arousals E_{ar} is a simple function of the required increase in body temperature from T_{tor} to euthermic levels, T_{eu}, and the specific heat capacity S of the hibernator's tissues[30]:

$$E_{ar} = (T_{eu} - T_{tor})S$$

The energetic cost of a complete torpor–arousal cycle, E_{bout}, is then

$$E_{bout} = E_{eu}(t_{eu}) + E_{tor}(t_{tor}) + E_{ar}$$

where t_{eu} and t_{tor} are time spent euthermic and torpid. The length of torpor bouts also varies dramatically with ambient temperature, presumably because of the thermal dependency of *TMR*[30]. Thus, t_{tor} reduces from maximum levels, $t_{tor\text{-}max}$, above and below $T_{tor\text{-}min}$ in accordance with increases in E_{tor}, such that

$$t_{tor} = t_{tor\text{-}max} Q_{10}^{(t_a - t_{tor\text{-}min}/10)}, \quad \text{if } T_a > T_{tor\text{-}min}$$

$$t_{tor} = t_{tor\text{-}max} + (T_a - T_{tor\text{-}min})k, \quad \text{if } T_a \le T_{tor\text{-}min}$$

where k is an analytical constant that yields equal values of t_{tor} for a given *TMR* above and below $T_{tor\text{-}min}$.

Finally, total hibernation energy requirements E_{winter} can be predicted for a given winter length t_{winter} according to

$$E_{winter} = \left(\frac{t_{winter}}{t_{bout}}\right) E_{bout}$$

where t_{bout} is the temperature-dependent duration of a torpor–arousal cycle.

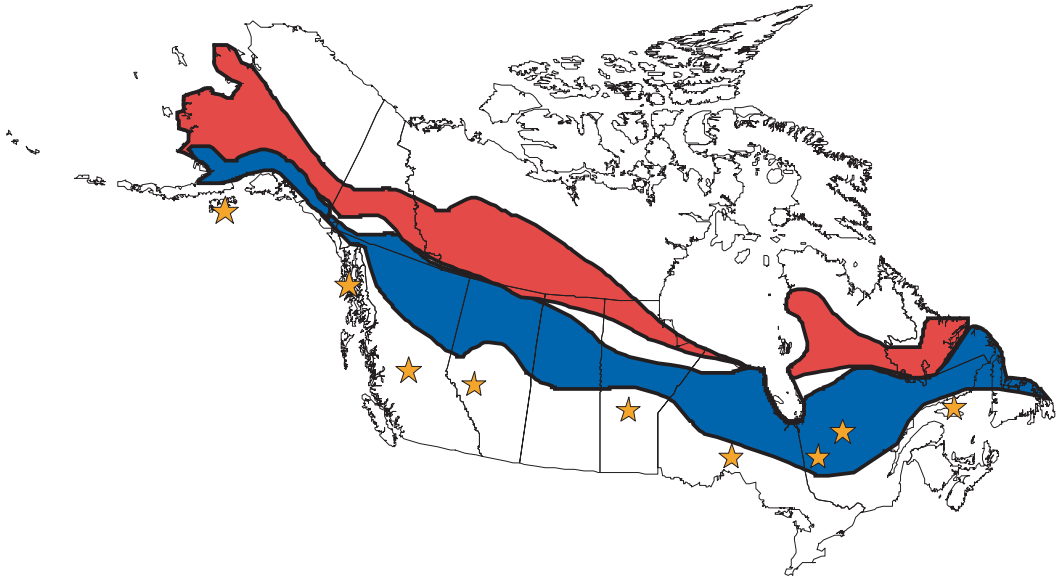

Figure 3 Observed and predicted *M. lucifugus* range distributions in northern North America. Confirmed northern locations of hibernacula (refs 10, 14, 19 and 29, and M. Gauthier, personal communication) are indicated with yellow stars, and the predicted distributional limit of hibernacula is indicated by the blue area; the width of the area represents variation in predictions resulting from cave temperatures exceeding average annual temperature by 0–2 °C, fat stores varying from 1.5 to 3.5 g, and all other parameters varying by up to ±5%. Thus, the lower margin of the blue zone indicates the limit beyond which to the south almost all bats could successfully hibernate, and the upper margin indicates the limit beyond which to the north almost no bats could successfully hibernate. Observed hibernacula approach and only marginally exceed the lower margin of this zone and there is a significant positive correlation between the latitude of observed hibernacula and the lower margin of this zone (predictions generated for each hibernaculum longitude, $n = 9$, $r = 0.93$, $P < 0.001$; intercept not significantly different from 0). The red area represents the predicted 2080 winter range limit of *M. lucifugus* due to global warming. Climate projections are based on the Hadley Centre coupled global climate model (HadCM2—GAX)[12]. The width of the red zone represents the same as does the blue zone.

conditions under which it hibernates. This species has a geographic range that extends into northern temperate and subarctic regions where individuals do not feed during winter[4] and instead rely completely on stored body fat during a prolonged hibernation period[9]. Because of morphological constraints and costs associated with fat storage, pre-hibernation fat reserves rarely exceed 40% of total body mass in hibernating mammals. For *M. lucifugus* in particular, the combination of aerial feeding (limiting the maximum size of a fat store), small body size (resulting in high mass-specific metabolic rate) and long winters in the northern part of its range impose severe constraints on the amount of energy available for hibernation[9]. Using a modelling approach applicable to all hibernating mammals, we estimate hibernation energy and fat requirements of *M. lucifugus* on the basis of the temperature dependency of euthermic metabolism, torpor metabolism, and the frequency and metabolic costs of arousals (Box 1). Because this species is an obligate insectivore that hibernates in caves and abandoned mines, both hibernaculum temperature and winter length can be readily estimated from climatic data (see Methods).

Our model predicts that hibernation energy requirements will be minimized at 2 °C and increase sharply with either an increase or decrease in hibernaculum temperature (Fig. 1). Energy requirements increase dramatically below 2 °C because in this temperature range, the energy costs of both torpor and euthermy increase as temperature decreases. Requirements increase more moderately above 2 °C because above this temperature the costs of torpor increase, but the costs of arousal and euthermy both decrease. Given a winter length of 193 days in the northern portion of the range of *M. lucifugus*[10], the temperature dependency of hibernation energetics should severely limit the range of temperatures where successful hibernation is possible. Hibernating at 2 °C for 193 days requires only 1.2 g of fat, but temperatures only 3 °C lower or 10 °C higher increase energy requirements threefold, exceeding the observed 3.5 g upper limit to fat stores[9] (Fig. 1). The validity of our model can be evaluated by comparing predicted combinations of winter length and hibernaculum temperature for which successful hibernation should be possible, with reported hibernacula temperatures of *M. lucifugus* at different latitudes. These empirical studies show that bats hibernate across a relatively wide temperature range within a geographic location[11], but that this range does not extend to regions predicted unsuitable by the model (Fig. 2).

The pronounced increase in hibernation energy requirements at low ambient temperatures, combined with constraints on the size of fat reserves at the onset of hibernation and the length of the hibernation season, permits application of our model to predict the northern biogeographical limit for *M. lucifugus* hibernation. So applied, our model predicts that the minimum fat stores typically accumulated by this species[9] are inadequate for successful hibernation throughout the northern portions of the Canadian provinces, and that maximum accumulated stores are inadequate throughout most of Alaska and the Canadian territories (Fig. 3). Confirmed northern hibernacula of *M. lucifugus* extend to mid-latitude regions of Canadian provinces and maritime-influenced areas of Alaska, where our model predicts successful hibernation by most individuals, but not into higher latitudes and continental regions, where our model predicts that successful hibernation is energetically impossible (Fig. 3). Energetic constraints at higher latitudes should be especially severe for juveniles, owing to their limited capacity to grow and fatten during a short active season[9].

The correspondence between predicted and observed hibernaculum microclimates (Fig. 2) and between predicted and observed northern hibernaculum localities (Fig. 3) provides strong evidence that the distribution of *M. lucifugus* is constrained by thermal effects on hibernation energetics. This mechanistic link between tempera-

ture and biogeography permits prediction of the future impacts of climate change. Current global climate models predict a 6–8 °C increase in average annual temperature throughout most of northern North America within the next 80 years[12]. On the basis of our model (see Methods), this climatic warming will result in a pronounced northward expansion of *M. lucifugus* (Fig. 3).

The success of this simple model, rooted in the fundamental energetics of the species, in predicting biogeographical distributions, demonstrates how the study of energetics can link climate to biogeography. Previous studies have demonstrated a correspondence between distributional temperature and several physiological processes[2], but have been unable to explain how these correspondences generate species range limits[7]. Establishing this link in *M. lucifugus*, using an approach that can be generalized to many other organisms that experience seasonal energetic bottlenecks, facilitates the use of bioenergetics to explain the present-day range boundaries and to predict the sensitivity of these boundaries to future climate change. The pronounced northward expansion of little brown bats predicted to occur within the next century provides a clear but singular example of the major impacts that human-induced climate change will have on the range limits of endotherms. Enhancing our understanding of the links between bioenergetics and biogeography in a wider diversity of species will improve our capacity to anticipate the biological impacts of global climate change. □

Methods

Model parameters and sensitivity

Parameter values for *M. lucifugus* were obtained from the literature (see Supplementary Information; see Box 1 for parameter definitions). Model sensitivity was first investigated by determining how independent variation in each parameter influenced our estimate of total winter energy requirements (E_{winter}) at $T_a = 0$ °C. The proportion of variation in each parameter reflected in variation in E_{winter} ('sensitivity') ranges from 0.01 to 0.77. For example, a 5% change in the value of $T_{tor\text{-}min}$ (sensitivity = 0.77) would alter our E_{winter} estimate by slightly less than 4%, whereas a 5% change in t_{ar} (sensitivity = 0.01) would alter E_{winter} by less than 0.1%. Sensitivity is highest for parameters related to the duration and energetic cost of torpor bouts (see Supplementary Information). The influence of combined variation of all terms was simulated by calculating E_{winter} at $T_a = 0$ °C using parameter values drawn randomly from a normal distribution with 99% of values within ±5% of the original parameter value. On the basis of 50,000 runs, the average deviation from our original E_{winter} prediction was only ±2% and the maximum was ±10%. Finally, the maximum potential deviation in our E_{winter} estimate at 0 °C resulting from a combined ±5% error in all parameters was determined analytically and was found to be ±17%. This sensitivity analysis ignores potential co-dependence among parameter values and thus will tend to overestimate the model's sensitivity.

Estimating winter length from climatic data

Because *M. lucifugus* is a nocturnal obligate insectivore[4] and near-freezing air temperatures inhibit insect activity[13], the minimum length of the hibernation period should approximate the period when average nightly minimum temperatures are less than 0 °C (night-time maximum temperatures would typically exceed this minimum by several degrees). Thus, climatological data from weather stations (Canadian Meteorological Centre, Climate and Water Information, Environment Canada (http://www.msc-smc.ec.gc.ca/climate); National Climatic Data Centre, National Oceanic and Atmospheric Administration, USA (http://lwf.ncdc.noaa.gov/oa)) can be used to predict how the duration of the hibernation period varies for *M. lucifugus* across its wide geographic distribution. Predictions for the onset, termination and total duration of hibernation at different latitudes, derived from our 0 °C nightly minimum assumption, correspond well with dates and durations reported in the literature[9,10,14–16], with an average absolute error of 5 days (range 0–13 days).

Estimating hibernaculum temperature from climatic data

Although the temperature profiles of caves and abandoned mines vary according to internal geometry, deep cave and mine temperatures generally approximate average annual temperature, whereas regions nearer to the entrance track winter temperatures more closely[17]. As a result, although the coldest sites available for hibernation are much less than annual average temperatures, the warmest sites exceed the annual average by only a few degrees, unless geothermally heated caves occur in the region[18]. We determined average annual temperature for each region, and assumed that the maximum hibernaculum temperature available in a given region could exceed this average by 0–2 °C; the width of the coloured areas in Fig. 3 incorporates the effect of this temperature range on the predicted northern distribution.

Climate forecasting

We obtained monthly mean and minimum temperature projections for 2020 from a global climate model (Hadley Centre Coupled Model 2 with aerosol simulation mean, HadCM2—GAX)[12] made available by the Canadian Climate Impacts and Scenarios (http://www.cics.uvic.ca) in collaboration with the Canadian Centre for Climate Modelling and Analysis and the Intergovernmental Panel on Climate Change. Because monthly temperature projections were available for a fine-scale georeferenced grid (cell size 2.50° latitude × 3.75° longitude), cave temperatures and winter lengths could be estimated for each cell, and entered into our model to evaluate the future potential for successful *M. lucifugus* hibernation across northern North America.

Received 21 March; accepted 22 April 2002; doi:10.1038/nature00828.

1. Gates, D. M. *Climate Change and Its Biological Consequences* 162–201 (Sinauer, Sunderland, Massachusetts, 1993).
2. Johnston, I. A. & Bennett, A. F. (eds) *Animals and Temperature: Phenotypic and Evolutionary Adaptation* (Cambridge Univ. Press, Cambridge, 1996).
3. Chown, S. L. & Gaston, K. J. Exploring links between physiology and ecology at macro-scales: the role of respiratory metabolism in insects. *Biol. Rev.* **74,** 87–112 (1999).
4. Fenton, M. B. & Barclay, R. M. R. *Myotis lucifugus. Mammal. Spec.* **142,** 1–8 (1980).
5. Rosenzweig, M. L. *Species Diversity in Space and Time* 8–48 (Cambridge Univ. Press, Cambridge, 1995).
6. Root, T. Environmental factors associated with avian distributional boundaries. *J. Biogeogr.* **15,** 489–505 (1988).
7. Canterbury, G. Metabolic adaptation and climatic constraints on winter bird distribution. *Ecology* **83,** 946–957 (2002).
8. Weiner, J. Physiological limits to sustainable energy budgets in birds and mammals—ecological implications. *Trends Ecol. Evol.* **7,** 384–388 (1992).
9. Kunz, T. H., Wrazen, J. A. & Burnett, C. D. Changes in body mass and fat reserves in pre-hibernating little brown bats (*Myotis lucifugus*). *Ecoscience* **5,** 8–17 (1998).
10. Fenton, M. B. Population studies of *Myotis lucifugus*. (Chiroptera: Vespertilionidae) in Ontario. *Life Sci. Contr., R. Ont. Mus.* **77,** 1–34 (1970).
11. Webb, P. I., Racey, P. & Speakman, J. R. How hot is a hibernaculum? A review of the temperatures at which bats hibernate. *Can. J. Zool.* **74,** 761–765 (1996).
12. Johns, T. C. *et al.* The second Hadley Centre couple ocean–atmosphere GCM: model description, spinup and validation. *Clim. Dyn.* **13,** 103–134 (1997).
13. Rainey, R. C. in *Insect Flight* (ed. Rainey, R. C.) 75–112 (Blackwell Scientific, Oxford, 1976).
14. Schowalter, D. B. Swarming, reproduction, and early hibernation patterns of *Myotis lucifugus* and *M. volans* in Alberta, Canada. *J. Mammal.* **61,** 347–350 (1980).
15. Whitaker, J. O. & Rissler, L. J. Winter activity of bats at a mine entrance in Vermillion County, Indiana. *Am. Midl. Nat.* **127,** 52–59 (1992).
16. Raesley, R. L. & Gates, J. E. Winter habitat selection by north temperate cave bats. *Am. Midl. Nat.* **118,** 15–31 (1986).
17. Dwyer, P. D. Temperature regulation and cave-dwelling in bats: an evolutionary perspective. *Mammalia* **35,** 424–455 (1971).
18. Bell, G. P., Bartholomew, G. A. & Nagy, K. A. The roles of energetics, water economy, foraging behaviour, and geothermal refugia in the distribution of the bat, *Macrotus californicus*. *J. Comp. Physiol. B* **156,** 441–450 (1986).
19. Parker, D. I., Lawhead, B. E. & Cook, J. A. Distributional limits of bats in Alaska. *Arctic* **50,** 256–265 (1997).
20. Twente, J. W. Environmental problems involving the hibernation of bats in Utah. *Proc. Utah Acad. Sci. Arts Lett.* **37,** 67–71 (1960).
21. Menaker, M. Hibernation–hypothermia: an annual cycle of response to low temperature in the bat *Myotis lucifugus*. *J. Cell. Comp. Physiol.* **59,** 163–173 (1962).
22. Pearson, E. W. Bats hibernating in silica mines in southern Illinois. *J. Mammal.* **43,** 27–33 (1962).
23. Davis, W. H. & Hitchcock, H. B. Notes on sex ratios of hibernating bats. *J. Mammal.* **45,** 475–476 (1964).
24. Henshaw, R. E. & Folk, G. E. Jr Relation of thermoregulation to seasonally changing microclimate in two species of bats (*Myotis lucifugus* and *M. sodalis*). *Physiol. Zool.* **39,** 223–236 (1966).
25. McManus, J. J. Activity and thermal preference of the little brown bat, *Myotis lucifugus*, during hibernation. *J. Mammal.* **55,** 844–846 (1974).
26. Nagorsen, D. W. Records of hibernating big brown bats (*Eptesicus fuscus*) and little brown bats (*Myotis lucifugus*) in Northwestern Ontario. *Can. Field Nat.* **94,** 83–85 (1980).
27. Brack, V. Jr & Twente, J. W. The duration of the period of hibernation of three species of vespertilionid bats. I. Field studies. *Can. J. Zool.* **63,** 2952–2954 (1985).
28. Thomas, D. W. The physiological ecology of hibernation in vespertilionid bats. *Symp. Zool. Soc. Lond.* **67,** 233–244 (1995).
29. Nagorsen, D. W. *et al.* Winter bat records for British Columbia. *Northwest. Nat.* **74,** 61–66 (1993).
30. Speakman, J. R. & Thomas, D. W. in *Bat Biology* (eds Kunz, T. H. & Fenton, M. B.) (Univ. Chicago Press, Chicago, in the press).

Supplementary Information accompanies the paper on *Nature*'s website (http://www.nature.com/nature).

Acknowledgements

We thank J. Umbanhowar for assistance with model sensitivity analysis as well as D. Kramer and K. McCann for comments on the presentation. This research was supported through a National Sciences and Engineering Research Council of Canada (NSERC) postdoctoral fellowship to M.M.H., and an NSERC research grant to D.W.T.

Competing interests statement

The authors declare that they have no competing financial interests.

Correspondence and requests for materials should be addressed to M.M.H. (e-mail: murray_humphries@hotmail.com).